ACKNOWLEDGMENT

The author wishes to thank D. M. Snider for helpful discussions, Prof. P. Penfield for allowing effective use of his circuit analysis program MARTHA, and C. Berglund for making many of the measurements.

REFERENCES

[1] W. J. Evans and G. I. Haddad, "A large signal analysis of IMPATT diodes," *IEEE Trans. Electron Devices*, vol. ED-15, pp. 708–717, Oct. 1968.

[2] M. Gilden and M. E. Hines, "Electronic tuning effects in the Read microwave avalanche diode," *IEEE Trans. Electron Devices (Special Issue on Semiconductor Bulk-Effect and Transit-Time Devices)*, vol. ED-13, pp. 169–175, Jan. 1966.

[3] W. T. Read, "A proposed high frequency negative resistance diode," *Bell Syst. Tech. J.*, vol. 37, pp. 401–466, Mar. 1968.

[4] H. K. Gummel and D. L. Scharfetter, "Avalanche region of IMPATT diodes," *Bell Syst. Tech. J.*, vol. 45, pp. 1797–1828, Dec. 1966.

[5] D. R. Decker, C. N. Dunn, and R. L. Frank, "Large-signal silicon and germanium avalanche-diode characteristics," *IEEE Trans. Microwave Theory Tech. (Special Issue on Microwave Circuit Aspects of Avalanche-Diode and Transferred Devices)*, vol. MTT-18, pp. 872–876, Nov. 1970.

[6] C. B. Swan, "IMPATT oscillator performance improvement with second harmonic tuning," *Proc. IEEE* (Lett.), vol. 56, pp. 1616–1617, Sept. 1968.

[7] C. A. Brackett, "Circuit effects in second-harmonic tuning of IMPATT diodes," *IEEE Trans. Electron Devices*, vol. ED-18, pp. 147–150, Mar. 1971.

[8] D. M. Snider, "A one-watt CW high-efficiency *X*-band avalanche-diode amplifier," *IEEE Trans. Microwave Theory Tech.* (Corresp.), vol. MTT-18, pp. 963–967, Nov. 1970.

[9] D. F. Peterson, "Characterization of an avalanche diode oscillator," M.S. thesis, Dep. Elec. Eng., Mass. Inst. Technol., Cambridge, Jan. 1969.

[10] W. E. Schroeder and G. I. Haddad, "Effect of harmonic and subharmonic signals on avalanche-diode oscillator performance," *IEEE Trans. Microwave Theory Tech.* (Corresp.), vol. MTT-18, pp. 327–331, June 1970.

[11] M. E. Hines, "Large signal noise, frequency conversion and parametric instabilities in IMPATT diode networks," to be published.

[12] D. H. Steinbrecher and D. F. Peterson, "Small-signal model with frequency-independent elements for the avalanche region of a microwave negative-resistance diode," *IEEE Trans. Electron Devices*, vol. ED-17, pp. 883–891, Oct. 1970.

[13] W. E. Schroeder, "Nonlinear properties of IMPATT diodes," Ph.D. dissertation, Univ. Michigan, Ann Arbor, 1972.

Large-Signal Equivalent Circuit for IMPATT-Diode Characterization and Its Application to Amplifiers

MADHU-SUDAN GUPTA

***Abstract*—A frequency-independent lumped equivalent circuit is proposed for characterizing the large-signal behavior of IMPATT diodes. It has five elements including a negative resistance, two of which are quadratic functions of the single-frequency RF voltage across the device. It is used for computer-aided analysis and the design of reflection-type negative-resistance amplifiers employing IMPATT diodes. The frequency response of the amplifier is calculated for different input power levels and the nature of the results is found to be in agreement with published experimental results.**

I. INTRODUCTION

A WEALTH of information is available in the literature on the design and analysis of reflection-type amplifiers, using negative-resistance devices such as tunnel diodes. The various techniques published can be classified into two groups depending upon the method used for characterization of the device. In one—the "time-domain method," the device is described by means of a time-domain i–v relationship $i=f(v)$ or $v=g(i)$, and given the instantaneous value of one of either v or i the other can be found. The function f (or g) is typically chosen as a cubic [1] or a power series [2]. This approach has been used extensively for tunnel-diode amplifier design and analysis. The method is not directly applicable to IMPATT diodes because their i–v relationship[1] is a nonlinear integro-differential equation which cannot be replaced by an instantaneous power-series relationship.

In the second method, which is the "frequency-domain method," the device is replaced by a nonlinear lumped impedance. This has also been used widely for tunnel-diode amplifier design [4]. Again, the results obtained for tunnel diodes cannot be extended to IMPATT diodes readily because, unlike tunnel diodes, the device impedance is not purely resistive, is a function of frequency over the operating range, and is nonlinear (signal dependent) under large-signal operating conditions.

Such characteristics of IMPATT diodes have severely limited the utility of many of the existing analyses of negative-resistance amplifiers and have necessitated the use of numerical methods. Further, the conventional computer-aided circuit-analysis programs are not sufficient for the analysis and design of amplifiers; they must be supplemented by numerical algorithms for solving carrier transport equations

Manuscript received March 5, 1973; revised May 4, 1973.

The author was with the Department of Electrical Engineering, Queen's University, Kingston, Ont., Canada. He is now with the Department of Electrical Engineering and the Research Laboratory of Electronics, Massachusetts Institute of Technology, Cambridge, Mass. 02139.

[1] For a sinusoidal voltage, the plot in the i–v plane shows a closed loop which depends upon signal amplitude and frequency [3].

describing the diode model [5]. The purpose of this work is to make both the frequency-domain methods and the readily available circuit-analysis programs applicable to the design of IMPATT-diode amplifiers by presenting a frequency-independent large-signal lumped equivalent circuit of the diodes.

A large number of investigations have been carried out on IMPATT-diode amplifiers, including two earlier attempts of Ku and Scherer [6] and Peterson and Steinbrecher [7], [8] to propose a lumped equivalent circuit for IMPATT diodes and use it for optimizing the gain bandwidth [6] and predicting the intermodulation distortion and gain compression [8] of an IMPATT-diode amplifier, respectively. It is shown below in Section II that neither of the earlier models can be used for amplifier circuit design or the calculation of amplifier gain in a given circuit over the *entire useful frequency range* of the diode, and therefore their utility is limited. A new equivalent circuit is therefore presented here. Numerical evaluation of the equivalent-circuit parameters for a computer-aided characterization of IMPATT diodes is briefly discussed in Section III. It is then shown in Section IV that the present equivalent circuit can be used for predicting the performance of IMPATT-diode amplifiers under given circuit conditions, and for amplifier circuit design. The nature of the results obtained using the equivalent circuit is found to be in agreement with the published experimental results.

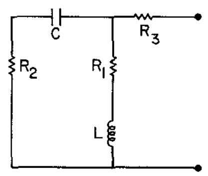

Fig. 1. Lumped frequency-independent equivalent circuit for IMPATT diode. R_2 is a negative resistance.

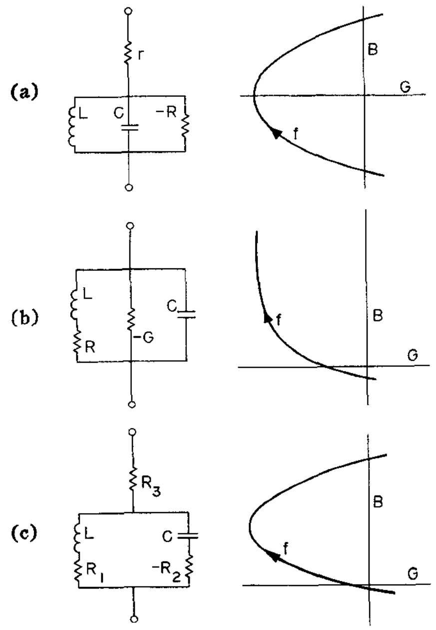

Fig. 2. Comparison of the frequency dependence of the IMPATT-diode admittance calculated from different frequency-independent equivalent circuits. (a) Ku and Scherer's model. (b) Peterson and Steinbrecher's model. (c) The model used in the present paper.

II. Comparison of Equivalent Circuits

A five-lumped-element frequency-independent negative-resistance small-signal equivalent circuit for an IMPATT diode has recently been proposed [9] and is shown in Fig. 1. The equivalent circuit is valid over approximately an octave band of frequency around the frequency of maximum negative conductance of the diode. The circuit elements constituting the equivalent circuit can be determined [9] either analytically, from a knowledge of the diode material, structural, and operating point parameters, or numerically, by fitting the equivalent-circuit admittance

$$Y_{\text{eq}}(\omega) = \frac{1 + j\omega C(R_1 + R_2) - \omega^2 LC}{(R_1 + R_3) + j\omega(L + R_1R_2C + R_1R_3C + R_2R_3C) - \omega^2 LC(R_2 + R_3)} \tag{1}$$

to the diode admittance $Y_D(\omega)$, which itself may have been determined experimentally or by an accurate small-signal analysis. This circuit will be extended here to serve as a large-signal equivalent circuit by allowing the elements to be nonlinear; in particular, a quadratic function of the RF voltage amplitude.

There are two major differences between the equivalent circuit proposed here and those of earlier authors mentioned previously. The first is clear from Fig. 2, where the frequency variation of admittance is shown in the admittance plane for the three equivalent circuits. For the circuit of Fig. 2(a), given by Ku and Scherer [6], the diode susceptance is zero at the frequency of maximum negative conductance which is not true for IMPATT diodes. Therefore, an amplifier circuit cannot be designed and the gain in a known circuit cannot be correctly predicted from this model. The circuit of Fig. 2(b), proposed by Steinbrecher and Peterson [7], has a negative conductance which is not band-limited (indeed, it increases monotonically with frequency), so that the frequency response and bandwidth cannot be correctly determined. The equivalent circuit is valid only in the limit of low frequencies. (It may also be useful to higher frequencies for IMPATT diodes with a p-i-n doping profile due to the nature of their admittance [10].) Finally, the admittance of the circuit of Fig. 2(c), proposed here, has a frequency dependence similar to that of an IMPATT diode over most of the negative conductance region [9].

The second difference lies in the method of accounting for the diode nonlinearity. Ku and Scherer have made no attempt to make the model nonlinear in order to match the large-signal behavior of the diode. Peterson and Steinbrecher [8] have replaced the negative resistance of the circuit of Fig. 2(b) by a driven current source and made the inductance L nonlinear, which they show to be valid in the limit of low frequencies. Presently, the nonlinear nature of the IMPATT diode is simulated by allowing the elements of the circuit of Fig. 2(c) to be dependent upon RF signal level.

III. Evaluation of Large-Signal Equivalent Circuit

Several authors have evaluated the large-signal admit-

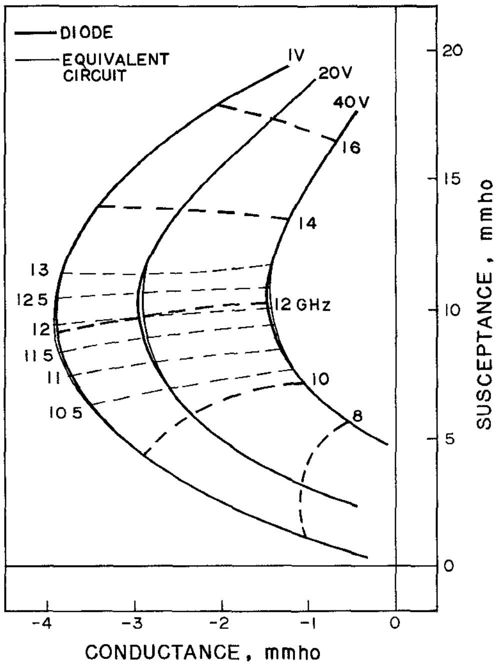

Fig. 3. Large-signal admittance of a silicon IMPATT diode (obtained by large-signal analysis) and of the equivalent circuit (with parameters given below) plotted in the admittance plane as a function of the frequency and the amplitude of a sinusoidal voltage assumed across the diode. The equivalent-circuit parameters are $R_{1ss}=32\ \Omega$, $R_2=-44\ \Omega$, $R_3=58\ \Omega$, $C=0.2$ pF, $L_{ss}=2.5$ nH, $r_1=10^{-2}/\mathrm{V}$, $r_2=8\times10^{-4}/\mathrm{V}^2$, $l_1=3\times10^{-3}/\mathrm{V}$, and $l_2=7\times10^{-5}/\mathrm{V}^2$.

tance of an IMPATT diode from analytical models [3], [10] and experimental measurements [11], [12]. A typical result is shown in Fig. 3, which was obtained by a numerical large-signal analysis of an X-band silicon IMPATT diode as in [13]. The figure shows the diode admittance plotted in the admittance plane as a function of the frequency and amplitude of a sinusoidal voltage assumed[2] across the diode:

$$V(t) = V_1 \sin \omega_1 t. \tag{2}$$

The 1-V curve in Fig. 3 may be taken as representing the small-signal diode admittance. The circuit elements in the equivalent circuit of Fig. 1 are therefore selected to yield a terminal admittance $Y_{eq}(\omega)$ closely agreeing with the diode small-signal admittance $Y_D(\omega)$, and it has been shown that very good agreement is achievable [9]. The five circuit element values given with the figure were obtained in this manner.

As the nature of the large-signal admittance (20- and 40-V curves in Fig. 3) is similar to the small-signal admittance (1-V curve), the equivalent circuit could also be selected for a good fit of $Y_{eq}(\omega)$ to the large-signal diode admittance. This implies that a change in diode admittance due to the presence of a large-signal voltage at the diode terminals can be incorporated in the equivalent circuit by changing some of the circuit parameter values. A nonlinear model will result if one or more of the five equivalent circuit elements are dependent upon this voltage. A good approximation to the large-signal behavior of the IMPATT-diode admittance was obtained by allowing both elements in the inductive branch of the circuit of Fig. 1 to be nonlinear. The element values are expressed as frequency-independent quadratic functions of the peak RF voltage across the diode to avoid parametric effects and simplify the calculations involved; thus

$$R_1 = R_{1ss}(1 + r_1V_1 + r_2V_1^2) \tag{3a}$$

$$L = L_{ss}(1 + l_1V_1 + l_2V_1^2) \tag{3b}$$

where R_{1ss} and L_{ss} are the small-signal values of the elements and r_1, r_2, l_1, and l_2 are the constants specifying the nonlinearity. Further, while the small-signal equivalent-circuit parameters were calculated for a good fit of $Y_{eq}(\omega)$ to the small-signal diode admittance, the nonlinearity constants must be calculated for a good fit of $Y_{eq}(V_1, \omega)$ to the large-signal diode admittance. The four constants were calculated here using the signal voltage dependence of the diode conductance G_D as the criterion of good fit.[3]

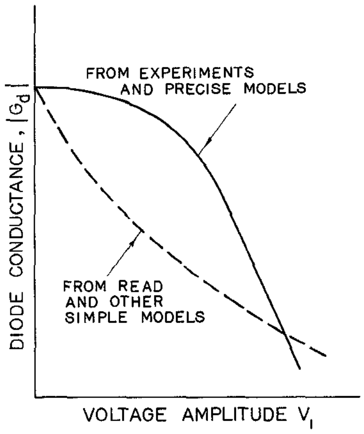

Fig. 4. Variation of the large-signal diode conductance G_D with the single-frequency RF voltage V_1 as calculated from different models and experiments.

The diode conductance G_D decreases with increasing RF voltage in a manner indicated by the solid curve in Fig. 4 (except at low frequencies close to avalanche frequency). This variation of G_D with V_1 was calculated by a large-signal analysis[4] at two separate frequencies within the frequency band of interest in the amplifier. The four constants of nonlinearity were so chosen that the voltage variation of equivalent-circuit conductance G_{eq} matches $G_D(V_1)$. The calculated constants and the equivalent-circuit admittance are given in Fig. 3, which shows that a good agreement between diode and equivalent-circuit large-signal admittance is possible. At large signals, the frequency range of validity of the model is somewhat reduced; however, it is still fairly accurate for frequen-

[2] The nature of the results does not change significantly under some alternative assumptions [14].

[3] It should be emphasized that the proposed equivalent circuit approximates only the terminal properties of the diode and is not unique; a different small-signal equivalent circuit with a different number of circuit elements could serve as the starting point; different elements could be made nonlinear under large-signal conditions; the nonlinear elements could be functions of the instantaneous, or some type of average value of, the signal voltage across, or the current through, either the diode or the element itself; and different criteria of "good fit" could be used. The accuracy and convenience of computation determine the choice.

[4] A precaution is necessary in obtaining an equivalent circuit for good fit to analytically evaluated large-signal diode admittance. Simple diode models [3] lead to a signal-dependent negative conductance, shown by the broken curve in Fig. 3, from which power saturation cannot be predicted. A more extensive model [13] or experimental results [11], [12], [15] are required for correct prediction of the large-signal behavior of IMPATT-diode amplifiers.

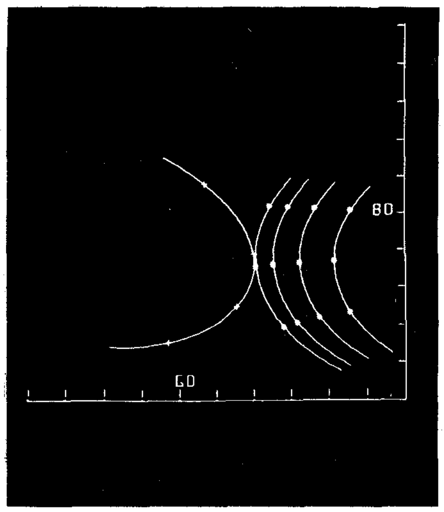

Fig. 5. Large-signal admittance calculated from the equivalent circuit and plotted on a computer-driven display terminal. Horizontal scale: 1 division = 1 mmho (conductance). Vertical scale: 1 division = 2.5 mmho (susceptance). The four right-hand side curves are for 1-, 10-, 20-, and 30-V amplitudes going from left to right; asterisks on the curves indicate frequencies of 10, 12, and 14 GHz from bottom to top. The left-hand-side curve shows the negative of circuit admittance Y_c plotted on the same scale; the four frequencies marked on the $-Y_c$ curve are 11, 11.5, 12, and 12.5 GHz starting from the top.

cies where the negative conductance is large (and where the diode is likely to be operated for large signals), as shown in Fig. 3. Note that the entire large-signal admittance plane plot of Fig. 3 need not be measured or calculated in order to determine the equivalent circuit; the small-signal admittance and the variation of diode conductance with RF voltage alone are sufficient.

The evaluation of the equivalent-circuit elements for a "good fit" to the calculated large-signal diode admittance $Y_D(\omega)$ was carried out numerically on a computer. As the visual judgment of the goodness of fit is adequate for all practical purposes, a real-time computer-driven display terminal was used to observe the diode admittance plot. An example of this calculation is presented in Fig. 5, which shows the large-signal admittance of the equivalent circuit (with nonlinear R_l and L) given by (1), plotted in the admittance plane as a function of frequency for three different RF voltage amplitudes. The subsequent task of amplifier circuit design can also be simplified by displaying the negative of the circuit admittance (to be discussed later) simultaneously as a function of frequency as shown in Fig. 5. This allows the designer to modify the circuit or diode parameters and observe the results in real time; in particular, the circuit tuning elements can be varied in order to determine a passive circuit suitable for the given amplifier specifications. An indication of the amplifier stability can also be obtained by observing whether the magnitude of the device small-signal conductance is always smaller than the circuit conductance.

IV. Application to IMPATT-Diode Amplifier

In this section, the large-signal equivalent circuit of an IMPATT diode will be used to determine the performance of an IMPATT-diode amplifier for a typical circuit and operating conditions. A schematic diagram of the circulator-coupled reflection-type IMPATT-diode amplifier considered here is shown in Fig. 6, which is self-explanatory. It will be assumed that 1) the diode is the X-band silicon IMPATT diode for which an

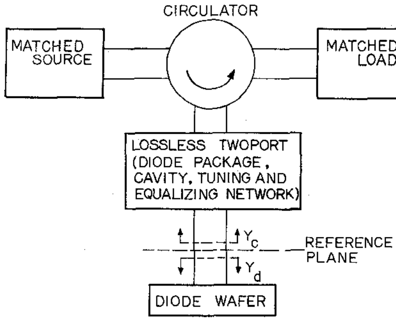

Fig. 6. Schematic diagram of a circulator-coupled reflection-type negative resistance amplifier.

equivalent circuit has been found in the previous section, 2) the circulator is broad-band and ideal, and 3) the circuit is a tunable coaxial cavity which has been described elsewhere [16].

Several papers reporting experimental measurements on IMPATT-diode amplifiers have appeared in the literature. As these measurements have been made on different diodes at various operating points and under different circuit conditions, a quantitative verification of the results computed here cannot be carried out; however, a qualitative agreement with published results will be pointed out in order to show the validity of the equivalent-circuit approach.

The amplifier is completely characterized if the nonlinear diode and the linear two-port (representing the diode package, cavity, and tuning arrangement) are modeled. The diode is characterized by the large-signal IMPATT-diode equivalent circuit described in the previous section. The linear two-port can be described by specifying the nature of the circuit; a tunable coaxial cavity is chosen because a model was available for this circuit [16]. Briefly, the model of the two-port consists of a lumped LC ladder network representing the diode package and a cascade of transmission-line sections together with lumped capacitances modeling the tuning elements and cavity. The two-port is thus assumed to be lossless. The circuit admittance Y_c, presented at the device terminals, can be calculated from this model [16].

The power gain of a reflection-type negative-resistance amplifier is given by the square of the reflection coefficient:

$$A = |\Gamma|^2 = \left|\frac{Y_c - Y_D^*}{Y_c + Y_D}\right|^2 \tag{4}$$

and the phase shift by the angle of the reflection coefficient, as

$$\phi = \underline{/\Gamma} = \tan^{-1}\left(\frac{\Gamma - \Gamma^*}{\Gamma + \Gamma^*}\right) \tag{5}$$

where the asterisk denotes the complex conjugate and Y_D and Y_c are the device and circuit admittances as seen at some arbitrarily chosen reference plane, looking towards and away from the device, respectively. For convenience, this reference plane will be chosen at the terminals of the diode wafer so that Y_c consists of linear passive elements only, and Y_D alone is signal dependent. The gain calculation therefore requires the calculation of Y_D and Y_c. The device admittance will be calculated from the large-signal equivalent circuit and the circuit admittance from the coaxial circuit model mentioned earlier.

With a sinusoidal voltage across the diode, as given by

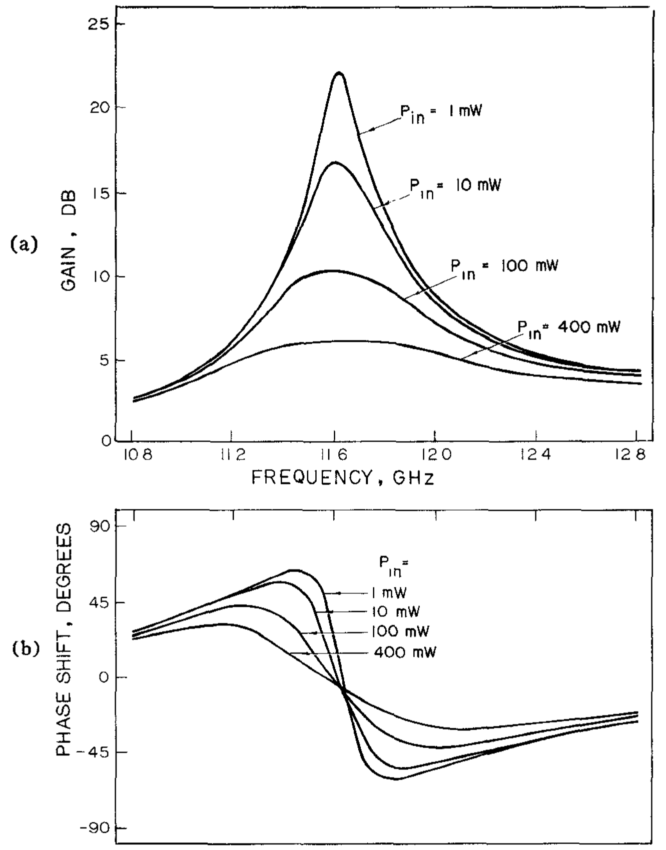

Fig. 7. Frequency-response of the IMPATT-diode amplifier in a coaxial circuit at different input power levels. (a) Gain. (b) Phase shift.

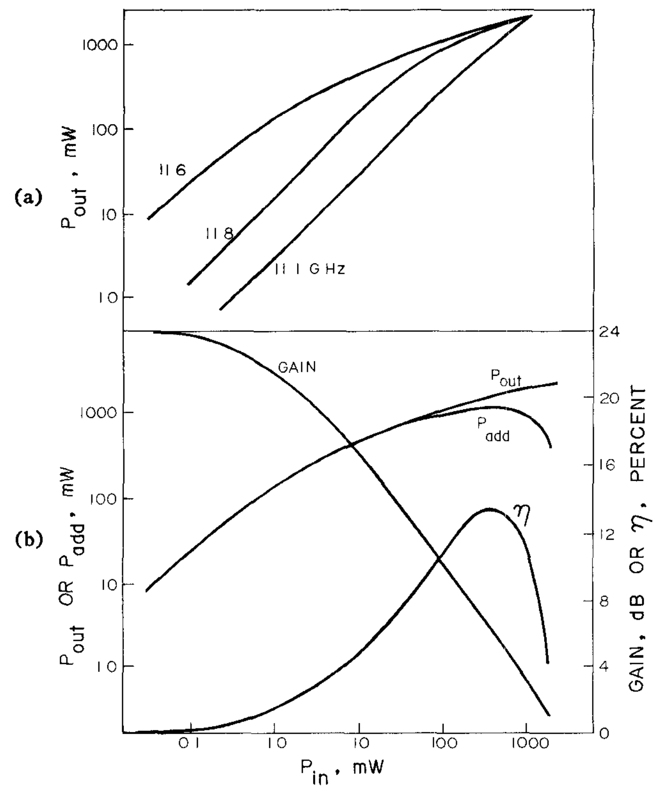

Fig. 8. (a) Variation of output power with input power at different operating frequencies for an IMPATT-diode amplifier in a coaxial circuit. (b) Variation of the power added, output power, gain, and efficiency with input power level at a single operating frequency (11.6 GHz) for the same amplifier.

(1), the RF power delivered by the diode is given by

$$P_{\text{add}} = \tfrac{1}{2}V_1^2 \, | G_d | \tag{6}$$

and is added to the input power P_{in}, so that the output power is given by

$$P_{\text{out}} = P_{\text{in}} + P_{\text{add}} = AP_{\text{in}} \tag{7}$$

which defines the power gain A of the amplifier. The efficiency of the amplifier will be defined as

$$\eta = \frac{P_{\text{add}}}{I_{\text{dc}}V_{\text{dc}}} \tag{8}$$

(where I_{dc} and V_{dc} are the dc current and voltage, respectively) and should be distinguished from the ratio of P_{out} to dc power.

The expressions for gain, phase shift, power added, power output, and efficiency, given in (4)–(8), were used for determining the performance of the amplifier at different frequencies and for various input power levels. The bandwidth of the amplifier depends upon the circuit tuning and input power level: Fig. 7 shows the calculated amplifier frequency response for a circuit with $Y_c(\omega)$ given in Fig. 5. Fig. 7(a) shows the response curve and the gain compression with increasing signal level, and is in agreement with the experimental results [1], [17], [18]. At lower frequencies, the circuit can be tuned such that the amplifier gain increases with increasing signal level (i.e., gain expansion occurs) for small input levels. The nature of the phase characteristic of Fig. 7(b) also agrees with the available experimental results within the amplifier passband [19]. The gain compression is largest and the phase shift is independent of signal level near the frequency of maximum gain. This is also apparent from the transfer characteristic at different fixed frequencies as shown in Fig. 8(a), which is of the nature observed experimentally [19], [20]. The performance of the amplifier at a fixed frequency is shown in Fig. 8(b). The added power (and hence the efficiency) reaches a maximum value equal to the maximum power available from the diode as a free-running oscillator, and falls upon further increasing the input as has been shown experimentally [1], [21]. The saturation of output power and the gain compression have also been experimentally observed [1], [18], [21].

IV. Conclusions

A frequency-independent nonlinear large-signal equivalent circuit has been proposed for IMPATT diodes and is shown to give a better approximation to the IMPATT-diode admittance than earlier models. This equivalent circuit has been used for calculating the performance of large-signal IMPATT-diode amplifiers. The nature of calculated results is in agreement with published experimental results, validating the use of equivalent circuit. The proposed equivalent circuit should be useful in computer-aided IMPATT-diode-amplifier design.

References

[1] C. W. Lee, "High power negative resistance amplifiers," *Microwave J.*, vol. 15, pp. 29–37, Feb. 1972.
[2] M. E. Hines, "Negative-resistance diode power amplification," *IEEE Trans. Electron Devices*, vol. ED-17, pp. 1–8, Jan. 1970.
[3] D. L. Scharfetter and H. K. Gummel, "Large-signal analysis of a silicon Read diode oscillator," *IEEE Trans. Electron Devices*, vol.

ED-16, pp. 64–77, Jan. 1969.

[4] M. E. Hines, "High-frequency negative-resistance circuit principles for Esaki diode applications," *Bell Syst. Tech. J.*, vol. 39, pp. 477–513, May 1960.

[5] R. W. Laton and G. I. Haddad, "The effects of doping profile on reflection-type IMPATT diode amplifiers," in *Proc. 1971 European Microwave Conf.* (Stockholm, Sweden, Aug. 1971), pp. A-5/1:1–5/1:4.

[6] W. H. Ku and E. F. Scherer, "Gain-bandwidth optimization of avalanche-diode amplifiers," *IEEE Trans. Microwave Theory Tech.* (*Special Issue on Microwave Circuit Aspects of Avalanche-Diode and Transferred Electron Devices*), vol. MTT-18, pp. 932–942, Nov. 1970.

[7] D. H. Steinbrecher and D. F. Peterson, "Small-signal model with frequency-independent elements for the avalanche region of a microwave negative-resistance diode," *IEEE Trans. Electron Devices*, vol. ED-17, pp. 883–891, Oct. 1970.

[8] D. F. Peterson and D. H. Steinbrecher, "Circuit model for characterizing the nearly linear behavior of avalanche diodes in amplifier circuits," *IEEE Trans. Microwave Theory Tech.*, vol. MTT-21, pp. 19–27, Jan. 1973.

[9] M. S. Gupta, "A small-signal and noise equivalent circuit for IMPATT diodes," *IEEE Trans. Microwave Theory Tech.* (Short Papers), vol. MTT-21, pp. 591–593, Sept. 1973.

[10] P. T. Greiling and G. I. Haddad, "Large-signal equivalent circuits of avalanche transit-time devices," *IEEE Trans. Microwave Theory Tech.* (*Special Issue on Microwave Circuit Aspects of Avalanche-Diode and Transferred Electron Devices*), vol. MTT-18, pp. 842–853, Nov. 1970.

[11] J. W. Gewartowski and J. E. Morris, "Active IMPATT diode parameters obtained by computer reduction of experimental data," *IEEE Trans. Microwave Theory Tech.*, vol. MTT-18, pp. 157–161, Mar. 1970.

[12] D. R. Decker, C. N. Dunn, and R. L. Frank, "Large-signal silicon and germanium avalanche-diode characteristics," *IEEE Trans. Microwave Theory Tech.* (*Special Issue on Microwave Circuit Aspects of Avalanche-Diode and Transferred Electron Devices*), vol. MTT-18, pp. 872–876, Nov. 1970.

[13] W. E. Schroeder and G. I. Haddad, "Nonlinear properties of IMPATT devices," *Proc. IEEE*, vol. 61, pp. 153–182, Feb. 1972.

[14] M. S. Gupta and R. J. Lomax, "A current-excited large-signal analysis of IMPATT devices and its circuit implications," *IEEE Trans. Electron Devices*, vol. ED-20, pp. 395–399, Apr. 1973.

[15] P. W. Braddock, "Experimental characterisation of avalanche-diode reflection amplifiers and locked oscillators," *Electron. Lett.*, vol. 7, pp. 42–44, Jan. 28, 1971.

[16] M. S. Gupta and R. J. Lomax, "A self-consistent large-signal analysis of a Read-type IMPATT diode oscillator," *IEEE Trans. Electron Devices*, vol. ED-18, pp. 544–550, Aug. 1971.

[17] D. M. Snider, "A one-watt CW high-efficiency X-band avalanche-diode amplifier," *IEEE Trans. Microwave Theory Tech.* (Corresp.), vol. MTT-18, pp. 963–967, Nov. 1970.

[18] Y. Takayama, "Power amplification with IMPATT diodes in stable and injection-locked modes," *IEEE Trans. Microwave Theory Tech.*, vol. MTT-20, pp. 266–272, Apr. 1972.

[19] G. B. Morgan and K. C. Siow, "Phase characteristics of microwave avalanche diode amplifiers," *Electron. Lett.*, vol. 8, pp. 280–281, June 1, 1972.

[20] H. Komizo, Y. Ito, H. Ashida, and M. Shinoda, "A 0.5-W CW IMPATT diode amplifier for high-capacity 11-GHz FM radio-relay equipment," *IEEE J. Solid-State Circuits*, vol. SC-8, pp. 14–20, Feb. 1973.

[21] W. Crowe and J. Sie, "The use of avalanche diodes in an amplifying mode to increase source output power," *Microwave J.*, vol. 12, pp. 67–69, Feb. 1969.

Analysis of Nonlinear Characteristics and Transient Response of IMPATT Amplifiers

H. J. KUNO

***Abstract*—Nonlinear characteristics, large-signal effects, and transient response of IMPATT amplifiers are analyzed leading to clear understanding of various nonlinear and large-signal phenomena which are often observed experimentally on IMPATT diodes operated as stable (linear) amplifiers or injection-locked oscillators. Effects of bandwidth on transient response of the IMPATT amplifiers as applied to phase-modulated signals and amplitude-modulated signals are investigated in detail. The relationship between the transition (switching) time and the amplifier bandwidth is derived. Capabilities and limitations of IMPATT diodes operated as stable amplifiers or injection-locked oscillators are discussed.**

Manuscript received January 24, 1973; revised April 6, 1973. This work was supported in part by the Air Force Avionics Laboratory, Air Force Systems Command, U.S. Air Force, Wright-Patterson AFB, Ohio.

The author is with Hughes Research Laboratories, Torrance, Calif. 90509.

I. Introduction

SINCE the discovery of microwave oscillation in a p-n junction diode biased into breakdown [1], [2], IMPATT (an acronym from IMPact ionization Avalanche Transit Time) devices have rapidly been developed into practical microwave power generators for system applications. In recent years, microwave power amplification with IMPATT diodes has become of great interest and importance for system applications.

Microwave power amplification can be achieved with an IMPATT diode operated as either a stable amplifier or as an injection-locked oscillator. This paper presents an analysis of nonlinear characteristics, large-signal effects, and transient response of both types of IMPATT amplifiers. The analysis